

International Journal of Engineering Research and Generic Science (IJERGS)

Available Online at www.ijergs.in

Volume -3, Issue-2, March - April 2017, Page No. 59 - 70

ISSN: 2455 - 1597

Dc Component Minimization by Using Virtual Capacitor on Photovoltaic Inverters by Integral Method S.Sandhya, G.Kumaraswamy, K.Kalyani, Godugula Mahesh

¹B.Tech scholars, Dept of EEE, SVS Institute of Technology, Hanamkonda, Warangal, T.S, India

M.Ramesh

²Assistant Professor, Dept of EEE, SVS Institute of Technology, Hanamkonda, Warangal, T.S, India

Abstract

In the power systems the dc component can affect the operating point of the transformers. The transformer cores are determined into unidirectional saturation with consequent larger excitation current. The transformer reduces the inrush currents and maintains required voltages but for low frequency (50 or 60 HZ) transformer is bulky, heavy, and expensive so its power loss brings down the overall system efficiency. Then the PV array is connected to the grid via a two level inverter three phase voltage source and an LCL filter is replaced instead of the transformer. The edge for dc module in the grid side ac currents is below 0.5% of the rated current. The dc component can cause dc-link voltage ripple, linefrequency power ripple and further second order harmonic in an ac current. The dc component injected to the grid can disturb the normal operation of the loads connected to the grid and causes torque ripple, extra loss in ac motors. To reduce the dc component in three phase ac currents the real solution is shown in this paper is to mimic the blocking capacitors used for the dc component reduction is called as virtual capacitor. The "virtual capacitor" is attained by adding an integral of the dc module in the current response path. The accurate extraction of the dc component can achieve the control, harmonic conditions and approved effective even under grid frequency variation. A proportional integral resonant controller is additional designed to regulate the dc and line frequency module in the current loop to deliver accurate control of the dc current. Here fuzzy logic is used for controlling compared to other controllers. The Simpered Systems tool has demonstrated that the joint system will at the same time inject maximum power from a PV unit and compensate the harmonic current drained by nonlinear loads.

Keywords: Controller, dc component, proportional integral resonant (PIR), transformer less three-phase PV inverters, virtual capacitor.

1. Introduction

Grid associated photovoltaic (PV) systems often include a line transformer between the grid and power converter. The transformer promises galvanic isolation between the grid and the PV systems. Further, it ensures that no direct current (dc) is injected to the grid. However, the low frequency (50 or 60 Hz) transformers large, heavy and expensive its power loss brings down the overall system efficiency. The dc component can have negative impacts on the power system in the following ways:

- 1) In the power system the dc component can affect the operating point of the transformers. With consequent larger excitation current the transformer cores are driven into unidirectional saturation. The service lifetime of the transformer is reduced as a result with additional increased hysteresis, eddy current losses and noise.
- 2) The dc component can circulate between inverter phase legs and inverters in a paralleled arrangement. The dc component circulation affect the loss distribution and even current among paralleled inverters.
- 3) The corrosion of grounding wire in substations is intensified

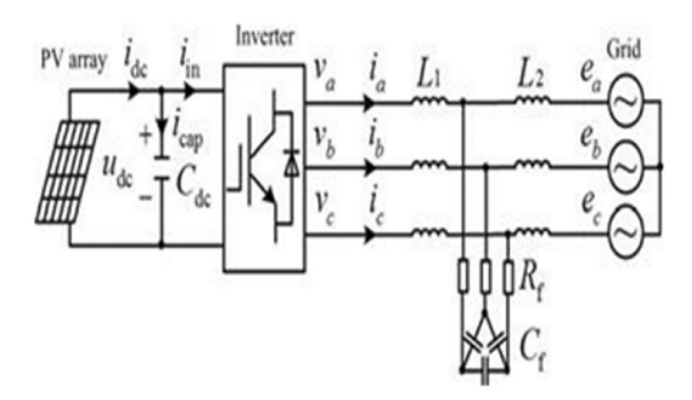


Figure 1: Transformer less three phase PV inverter system.

In the proposed control plan, an exact dc component quantity and extraction is critical. Here several devices can be used to amount the dc module, e.g., by shunt resistors, voltage transformers, mutual coupled inductors, and integral methods, etc. Among them, only the integral methods do not need additional hardware. So a new integral method based on the sliding window double time and iteration algorithm integral is presented. This technique is active in the extraction of the dc module even for currents with frequency fluctuations and harmonics

2. Impact Of The DC Components On PV Systems

A typical three phase transformer less PV inverter system is shown in above figure. The PV array is connected to the grid via three phase voltage source two level inverter and an LCL filter. The capacitors of the LCL filter are configured with a delta or star connection. In this paper, to reduce the required capacitor and cost a delta connection is used as *opposed to the star connection*, which has the benefit of smaller short-circuit current. The dual closed loop control strategy comprises a current and a dc-link voltage loop in the synchronous rotational frame, is a common control strategy in three phase PV inverters

$$\begin{cases} Fa = Fa0 + Fa1 \\ Fb = Fb0 + Fb1, \\ Fc = Fc0 + Fc1 \end{cases} \begin{cases} F\alpha = F\alpha0 + F\alpha1 \\ F\beta = F\beta0 + F\beta1 \end{cases}, \begin{cases} Fd = Fd0 + Fd1 \\ Fq = Fq0 + Fq1 \end{cases}$$

$$(1)$$

Where the subscript 0 denotes the dc component and the subscript 1 denotes the line-frequency

Component. If there are dc components in the abc coordinate, they will also exist in the form of dc or line frequency components in \square and dq coordinates, respectively. In a threphase three-wire system, there is no current flowing through the neutral point and hence the line frequency is

$$\begin{cases} Fa0 = Fb0 + Fc0 = 0 \\ Fa1 = Fb1 + Fc1 = 0. \end{cases}$$
 (2)

With (1) and (2), the coordinate transformations of the dc components from abc coordinate to and dq coordinate can be expressed as

$$\begin{pmatrix} Fa0 \\ F\beta0 \end{pmatrix} = \frac{2}{3} \begin{pmatrix} 1 - \frac{1}{2} - \frac{1}{2} \\ 0 \frac{\sqrt{3}}{2} - \sqrt{3/2} \end{pmatrix} \cdot \begin{pmatrix} Fa0 \\ Fb0 \\ Fc0 \end{pmatrix} = \begin{pmatrix} Fa0 \\ \frac{\sqrt{3}}{3Fb0} - \sqrt{3}/3Fc0 \end{pmatrix}$$

$$\begin{pmatrix} Fd1 \\ Fq1 \end{pmatrix} = \frac{2}{3} \begin{pmatrix} \cos\theta\sin\theta \\ -\sin\theta\cos\theta \end{pmatrix} \cdot \begin{pmatrix} 1 - \frac{1}{2} - \frac{1}{2} \\ 0 \frac{\sqrt{3}}{2} - \frac{\sqrt{3}}{2} \end{pmatrix} *$$

$$\begin{pmatrix} Fa0 \\ Fb0 \\ Fc0 \end{pmatrix} = \begin{pmatrix} Fa0\cos\theta + \frac{\sqrt{3}}{3} [Fa0 - Fco]\sin\theta \\ \frac{\sqrt{3}}{3} [Fb0 - Fco]\cos\theta - Fa0\sin\theta \end{pmatrix}$$

$$(4)$$

Where is the angle between the dq coordinate and abc coordinate for example, the grid angle in a grid voltage oriented vector control. Sin (3) and (4) the coordinate transformation, Fa0, Fb0and Fc0 (dc components) in the stationary abc frame can be transformed into F

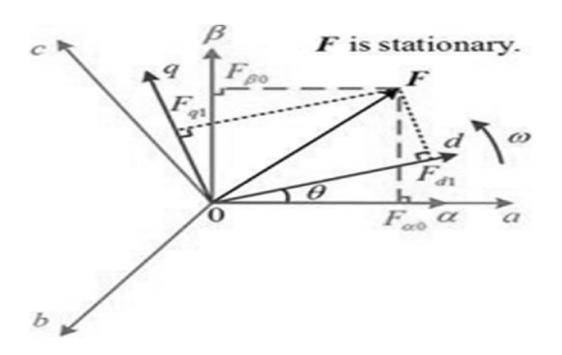


Figure 2: Coordinate transformation of dc components.

$$\begin{split} P_{ac} &= 3/2 \begin{bmatrix} Ud \\ Uq \end{bmatrix} T. \begin{bmatrix} Id \\ Iq \end{bmatrix} = 3/2 \begin{bmatrix} ud \, 0 + ud \, 1 \\ uq \, 0 + uq \, 1 \end{bmatrix} T. \begin{bmatrix} id \, 0 + id \, 1 \\ iq \, 0 + iq \, 1 \end{bmatrix} \\ &= \frac{3}{2} \begin{bmatrix} ud \, 0id \, 0 + q \, 0iq \, 0 + \\ DC \ component \\ + ud \, 0id \, 1 + ud \, 1id \, 0 + uq \, 0iq \, 1 + uq \, 1iq \, 0 + \\ Line - frequency \ fluctuation \\ ud \, 1id \, 1 + uq \, 1i \, 1 \\ 2nd \ fluctuation \\ \end{bmatrix} \end{split}$$

(5)

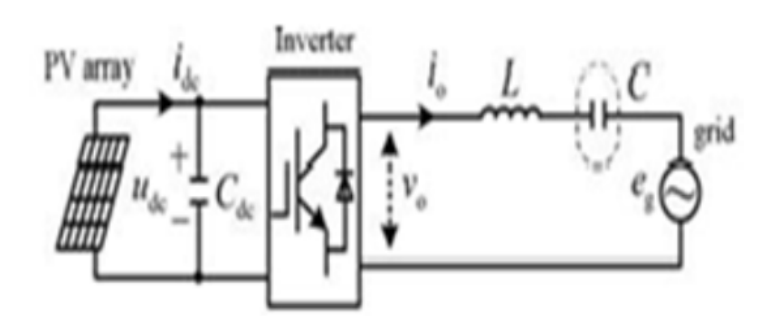


Figure 3: Circuit diagram of a single-phase grid-connected PV inverter with the blocking capacitor

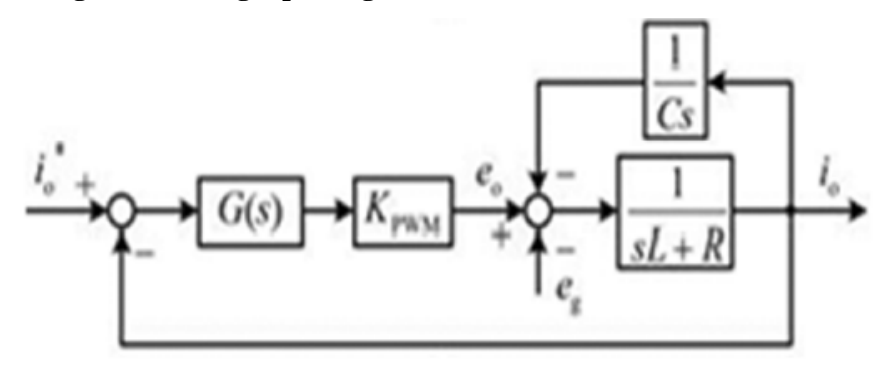


Figure 4: Current control loop diagram,

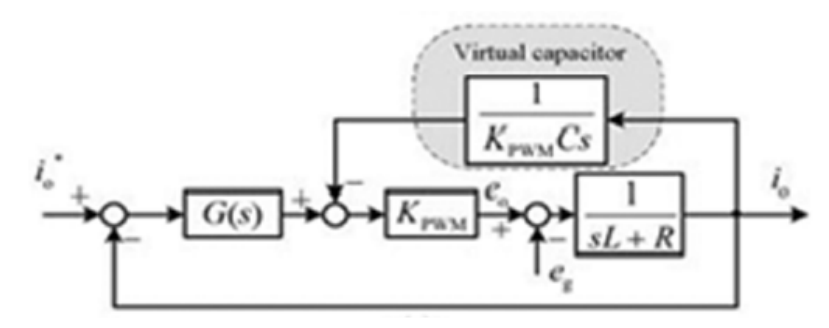


Figure 5: Equivalent transformation of the current control loop with virtual capacitor concept.

$$q_{ac} = 3/2 \begin{bmatrix} Ud \\ Uq \end{bmatrix} T * \begin{bmatrix} Id \\ Iq \end{bmatrix} = 3/2 \begin{bmatrix} ud0 + ud1 \\ uq0 + uq1 \end{bmatrix} T * \begin{bmatrix} id0 + id1 \\ iq0 + iq1 \end{bmatrix}$$
 (T = transpose)

$$=\frac{3}{2}\begin{bmatrix} ud\,0id\,0+q0iq\,0+\\ DC\,\,COMPONENT\\ +ud\,0id\,1+ud\,1id\,0+uq\,0iq\,1+uq\,1iq\,0+\\ LINE-FREQUENCY\,\,FLUCTUATION\\ ud\,1id\,1+uq\,1iq\,1\\ 2nd\,\,FLUCTUATION \end{bmatrix}$$

(6)

$$p_{ac} = \frac{3}{2} \begin{pmatrix} ud \, 0id \, 0 \\ DC \, component \\ +ud \, 0id \, 1 + ud \, 1id \, 0 \\ Line - \, frequency \, fluctuation \end{pmatrix}$$

$$q_{ac} = \begin{pmatrix} uq1id0 - ud0iq1 \\ Line - frequency fluctuation \end{pmatrix}$$
(7)

As shown, both the active and reactive power contains a line frequency, a constant dc power and a second order power fluctuation due to the dc component in the current and voltage undesired. Further, with grid voltage orientated vector control under unity power factor operation for PV applications, where uq0 = 0, iq0 = 0, (5) and (6) can be simplified as (7) f assuming the second order fluctuations is negligible compared to the other two components.

3. Existing System

There are many problems related to Transformer less structures, like dc element within the electrical converter output (grid) current, ground run current (due to common-mode voltage and parasitic capacitance), and also the voltage-level mate between the electrical device (inverter) and grid. Among them, the dc element will have an effect on the normal system operation and cause safety issues. Standards have so been established in several countries to limit the extent of the dc element

4. Disadvantage of Existing System

The dc component can have negative impacts on the power system in the following ways [9], [11]:

- 1) The dc component can affect the operating point of the transformers in the power system. The transformer cores are driven into unidirectional saturation with consequent larger excitation current. The service lifetime of the trans-former is reduced as a result with further increased hysteresis and eddy current losses and noise.
- 2) The dc component can circulate between inverter phase legs as well as among inverters in a paralleled configuration. The dc component circulation affects the even current and loss distribution among paralleled inverters.
- 3) The dc component injected to the grid can affect the nor-mal operation of the loads connected to the grid, for example, causing torque ripple and extra loss in ac motors.
- 4) The corrosion of grounding wire in substations is intensified due to the dc component.

5. Minimization Of Dc Component In Three-Phase Grid-Connected PV Systems

To block the dc component put a capacitor C in series with the ac side of the inverter However, in order to reduce the capacitive reactance at other frequencies, the value of the capacitor must be large; it increases the size and cost of the system. This series capacitor may also disturb the system dynamic response and reduce transmission efficiency. However,

the physical capacitor is replaced by software based method and advanced control strategy mimics the operation of the series capacitor in a single phase PV system

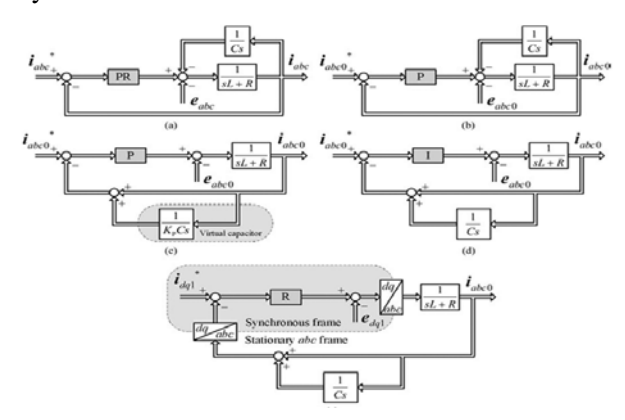


Figure 6: Virtual capacitor implementation for a three-phase PV inverter: (a) current control loop in stationary ab-c frame, (b) dc component control loop in stationary a-b-c frame, (c) equivalent transformation of the dc component control loop with virtual capacitor, (d) dc component control loop based on an integral (I) controller, and (e) dc component control loop in a mixed frame (d-q and a-b-c).

Where vo and io are the inverter output voltage and current, eg is the gird voltage; Vo(s), Io(s) and Eg(s) are the Laplace transforms of vo, ioand eg in the frequency domain, L is the filter inductance; R is the line equivalent resistance and C is the blocking capacitor. Substituting the operators in (10) with $j\Box$, I0 ($j\Box$) equals zero when \Box = 0(dc). This indicates that the blocking capacitor can minimize the dc component effectively.

6. Proposed System

A. Capacitor Concept Of Single-Phase grid-Connected PV Inverters Virtual

One way to block the dc component is to put a capacitor *C* in series with the ac side of the inverter. However, in order to reduce the capacitive reactance at other frequencies, the capacitor value needs to be large, which increases the size and cost of the system. This series capacitor may also affect the system dynamic response and reduce transmission efficiency. Nevertheless, the physical capacitor can be re-placed by software-based method and advanced control strategy which mimics the operation of the series capacitor in a single-phase PV system

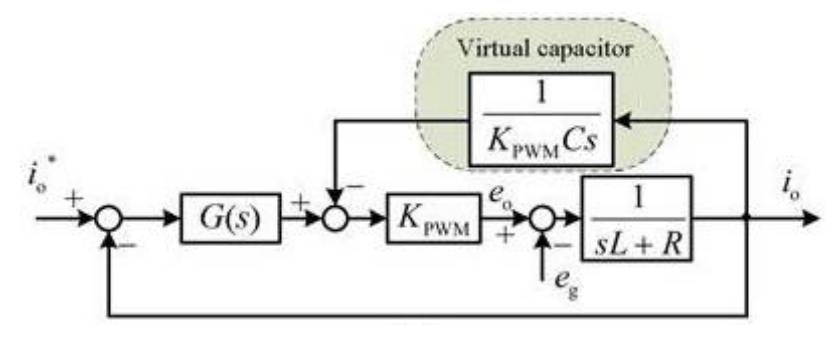
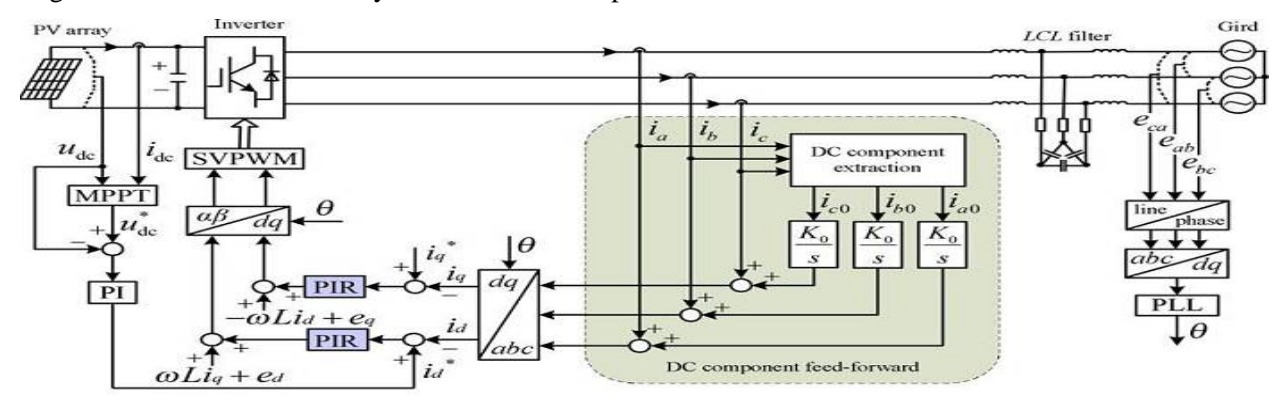


Figure 7: Equivalent transformation of the current control loop with virtual capacitor concept

DC Component Extraction by Using integral Method

In the control strategy an accurate dc component measurement and extraction is the key to implement the virtual capacitor concept and achieve the overall dc component minimization. Compared with the ac component, the dc component is very

small and an accurate dc component extraction is challenging. In PV inverters, the Hall-effect current sensors are widely used to measure the ac-side currents (including both ac and dc components) due to their smaller size, isolated output, and wide bandwidth (e.g., from dc to several hundred kilohertz). In this paper, an integral method based on the sliding window iteration algorithm is used to accurately extract the dc component from the ac-side currents.



On the sliding window iteration algorithm is used to accurately extract the dc component from the ac-side currents. Taking the ac-side Phase A current ia, for example, ia can be expressed as in (1) if considering both the component and other ac components of different frequencies (e.g., harmonics)

ia = ia0 +
$$\Sigma$$
 Ih sin (2 π hf1 t + ϕ h) ---- (1)
h = 1, 2, 3•••

where ia0 is the dc component, f1 is the line frequency. Ih, hf1, and ϕ h are the amplitude, frequency, and phase angle of the fundamental and harmonic components. Averaging the integration of (1) in the interval from t0 to t0 + T yields

$$\frac{1}{T} \int_{t_0}^{t_0+T} i_a dt = \frac{1}{T} \left[\int_{t_0}^{t_0+T} i_{a0} dt + \int_{t_0}^{t_0+T} \sum_{h=1,2,3\cdots} I_h \sin(2\pi h f_1 t + \varphi_h) dt \right].$$
(8)

When T = T1 = 1/f1, the second term in the right side of (2) becomes

$$\int_{t_0}^{t_0+T_1} \sum_{h=1,2,3...} I_h \sin(2\pi h f_1 t + \varphi_h) dt = 0.$$
(9)

Hence, with (2) and (3), the dc component ia0 can be obtained by, The next step is to implement the expression in (4) to obtain the dc component ia0 accurately without significant calculation burden. If assuming the number of sampling times in a fundamental period (T1) is N, dt in (4) can be substituted by the sampling interval t and t = T 1/N. If τ is defined as t/N, then Ia ($k\tau$) is the kth sampling value. Substituting the definite integration in (4) by the accumulation of the integrand, the discrete expression of ia0 is given by

$$i_{a0} = \frac{1}{N\Delta t} \sum_{k=0}^{N-1} i_a(k\tau) \Delta t = \frac{1}{N} \sum_{k=0}^{N-1} i_a(k\tau).$$
(10)

To achieve a real-time dc component extraction, (5) should accumulate the sampling values for N-1 times in one fundamental period. The amount of calculation is therefore significant given a high sampling frequency. To decrease the amount of calculation

$$i_{a0} = \frac{1}{N} \sum_{k=N_{\text{cur}}-N+1}^{N_{\text{cur}}} i_a(k\tau)$$

$$= \frac{1}{N} \sum_{k=N_{\text{cur}}-N}^{N_{\text{cur}}-1} i_a(k\tau) - i_a[(N_{\text{cur}}-N)\tau] + i_a(N_{\text{cur}}\tau)$$
(10)

where Ncur is the sliding pointer which represents the current sampling point. After completing the summation of one fundamental period for initialization

PIR Controller Design

As mentioned, when taking the dc component in the ac-side currents into account, the current loop in the dq frame is composed of both a dc component and a line-frequency component (negative sequence). The dc component in the rotational frame comes from the line-frequency ac components in the phase currents. The line-frequency component in the rotational frame comes from the dc component in the phase currents.

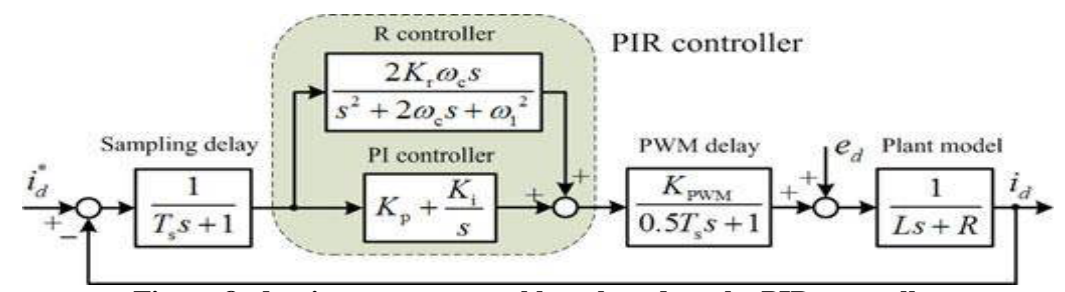


Figure 8: d-axis current control loop based on the PIR controller

To provide an effective control for both dc and line-frequency signals in the dq frame, a proportional-integral-resonant (PIR) controller is used. Taking the d-axis current control loop, for example, considering the sampling delay and the PWM delay, the current control loop based on the PIR controller where Ts is the sampling period, Kp is the proportional gain, Ki is the integral gain, and Kr is the resonant gain. $\omega 1$ is thereso-nant (center) frequency of the R controller, which is the same as the line frequency in this case. ωc is the cutoff frequency of the R controller to reduce the sensitivity against the slight frequency variations. the PI controller is used to regulate the dc component transformed from the fundamental currents. The Controller is used to regulate and minimize the line-frequency component transformed from the dc component. The parameters of the PI controller should be set to guarantee a good dynamic and steady-state performance of the current loop. The parameters of the R controller are set for the dc component minimization. An infinite gain at the resonant frequency of the R controller can eliminate the steady-state error. In the improved R

controller with $2\omega c$ added to the denominator as shown in Fig. 3, the gain at the resonant frequency is limited yet with improved performance under line-frequency fluctuation. Nevertheless, the gain can be adjusted by Kr. Regarding ωc , smaller ωc provides better frequency selectivity but difficult for digital implementation. Larger ωc leads to a wider bandwidth around the resonant frequency and a better robustness for the frequency deviation. However, the gain at the resonant frequency will be lower with a subsequent larger steady-state error.

7. Simulation Results

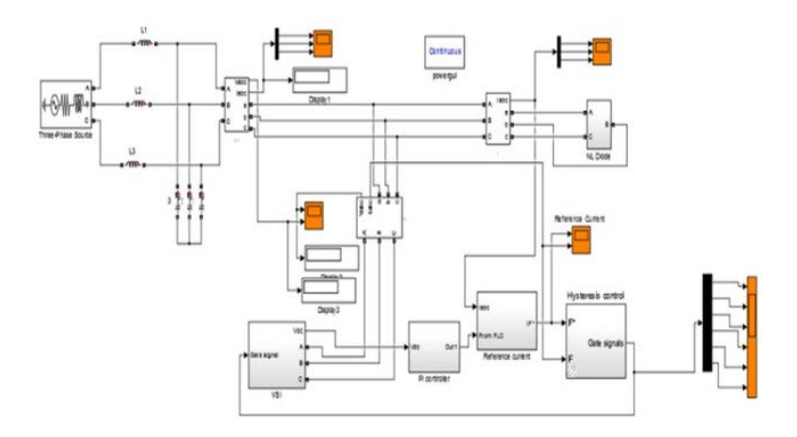


Figure 9: Simulation Diagram Change the Total Circuit

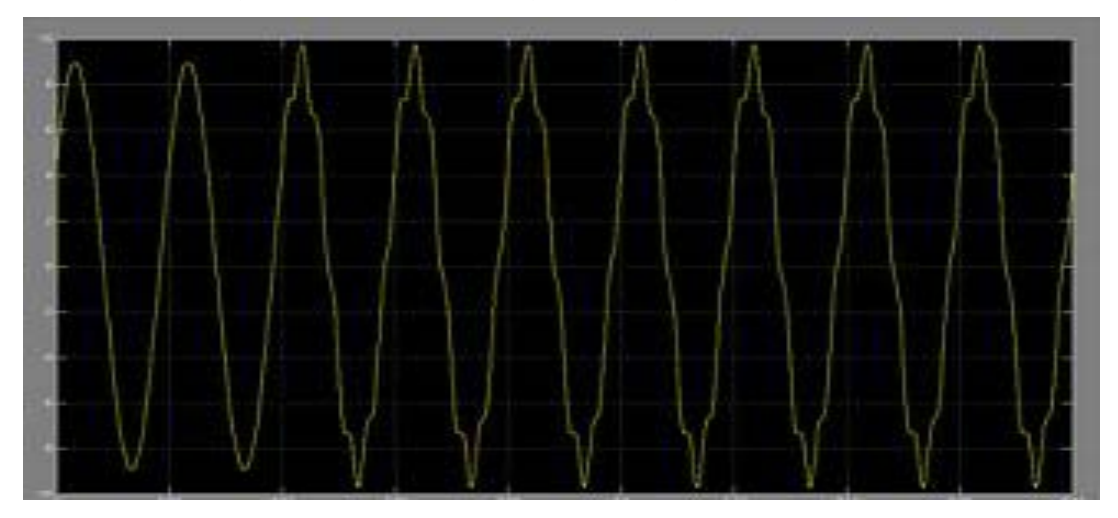


Figure 10: Grid current waveforms with DC component

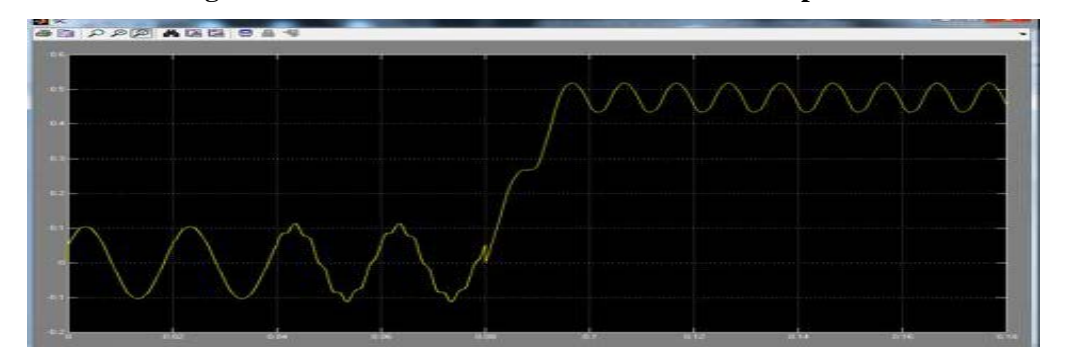


Figure 11: Minimized dc component of Grid current waveforms by single integral

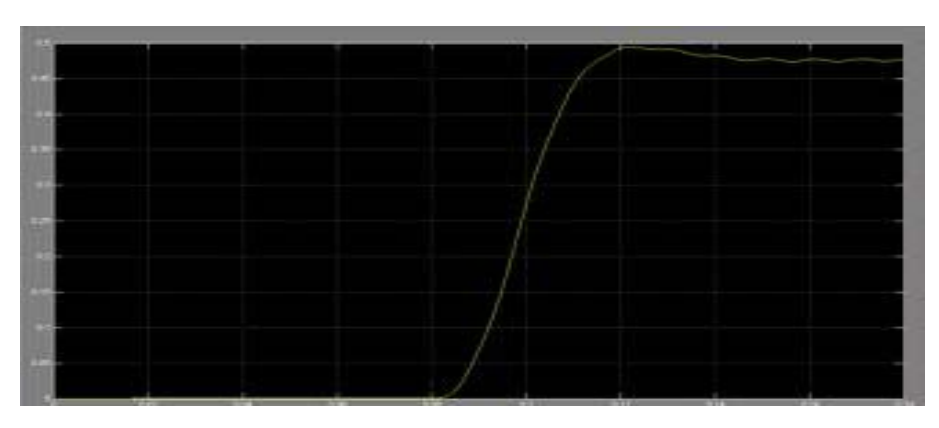


Figure 12: Minimized dc component of Grid current waveforms by double integral.

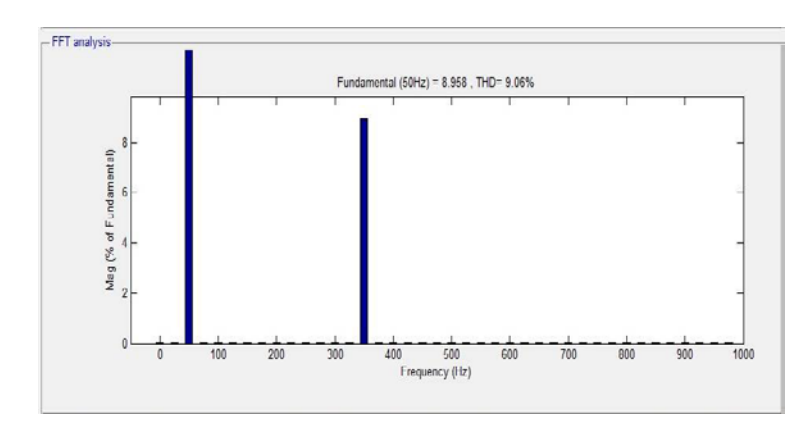


Figure 13: THD = 9.06%

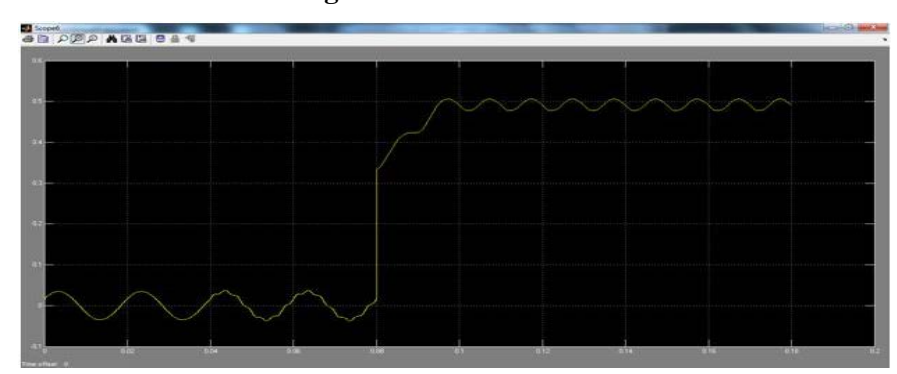


Figure 14: Minimized dc component of Grid current waveforms by single integral with fuzzy controller



Figure 15: Minimized dc component of Grid current waveforms by double integral with fuzzy controller

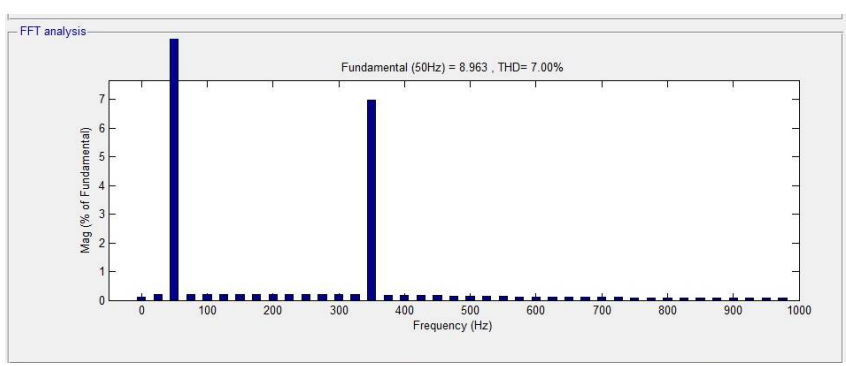


Figure 16: THD = 7.00%

8. Conclusion

This project has presented an effective method to minimize the dc component in a three-phase Transformer less grid connected PV system. The dc component can introduce line-frequency power ripple in the system and further cause dclinkvoltage ripple and second-order harmonics in the ac currents. A "virtual capacitor" approach has been implemented to minimize the dc component via a feed-forward of the dc component. The dc component can be accurately obtained using the sliding window iteration and double time integral even under frequency variation and harmonic conditions. APIR controller has been designed to enable the precise regulation of both the dc and line-frequency components in the dq frame. The proposed method can be well adopted in the existing PV systems for dc component minimization using the sliding window iteration and double time integral even under frequency variation and harmonic conditions for dc-component extraction and Minimization of dc-component feed forward term as well as the resonant controller in the current control loops.

9. References

- [1] R. Gonzalez, E. Gubia, J. Lopez, and L. Marroyo, "Transformer less single-phase multilevel-based photovoltaic inverter," IEEE Trans.Ind. Electron., vol. 55, no. 7, pp. 2694–2702, Jul. 2008.
- [2] S. B. Kjaer, J. K. Pedersen, and F. Blaabjerg, "A review of single-phase grid-connected inverters for photovoltaic modules," IEEE Trans.Ind. Appl., vol. 41, no. 5, pp. 1292–1306, Sep./Oct. 2005.
- [3] E. Koutroulis and F. Blaabjerg, "Design optimization of transformer less grid-connected PV inverters including reliability," IEEE Trans.Power Electron., vol. 28, no. 1, pp. 325–335, Jan. 2013.
- [4] B. Gu, J. Dominic, J. Lai, C. Chen, T. LaBella, and B. Chen, "High reliability and efficiency single-phase transformer less inverter for grid-connected photovoltaic systems," IEEE Trans. Power Electron., vol. 28, no. 5, pp. 2235–2245, May 2013.
- [5] S. V. Araujo, P. Zacharias, and R. Mallwitz, "Highly efficient single-phase transformer less inverters for grid-connected photovoltaic systems," IEEE Trans. Ind. Electron., vol. 57, no. 9, pp. 3188–3128, Sep. 2010.
- [6] O. Lopez, F. D. Freijedo, A. G. Yepes, P. Fernandez-Comesaa, J. Malvar, R. Teodorescu, and J. Doval-Gandoy, "Eliminating ground current in a transformer less photovoltaic application," IEEE Trans. Energy Convers., vol. 25, no. 1, pp. 140–147, Mar. 2010.

- [7] V. Salas, E. Ol'ıas, M. Alonso, and F. Chenlo, "Overview of the legislation of DC injection in the network for low voltage small gridconnectedPV systems in Spain and other countries," Renewable Sustainable Energy Rev., vol. 12, no. 2, pp. 575–583, Feb. 2008.
- [8] B. Wang, X. Guo, H. Wu, Q. Mei, and W. Wu, "Real-time DC injection measurement technique for transformer less PV systems," in Proc.
- IEEE 2nd Int. Symp. Power Electron. Distrib. Generation Syst., Hefei, China, Jun. 2010, pp. 980–983.
- [9] W. Li, L. Liu, T. Zheng, G. Huang, and S. Hui, "Research on effects of transformer DC Bias on negative sequence protection," in Proc. Int. Conf. Adv. Power Syst. Automat. Protection, Beijing, China, Oct. 2011, pp. 1458–1463.
- [10] A. Ahfock and A. J. Hewitt, "DC magnetisation of transformers," IEE Proc.-Electr Power Appl., vol. 153, no. 4, pp. 601–607, Jul. 2006.
- [11] M. A. S. Masoum and P. S. Moses, "Impact of balanced and unbalanced direct current bias on harmonic distortion generated by asymmetric three-phase three-leg transformers," IET Electr. Power Appl., vol. 4, no. 7, pp. 507–515, Jul. 2010.
- [12] F. Berba, D. Atkinson, and M. Armstrong, "A review of minimization of output DC current component methods in single-phase grid connected inverters PV applications," in Proc. 2nd Int. Symp. Environ. Friendly Energies Appl., Tyne, U.K., Jun. 2012, pp. 296–301.
- [13] M. Armstrong, D. J. Atkinson, C. M. Johnson, and T. D. Abeyasekera, "Auto-calibrating DC link current sensing technique for transformer less, grid connected, H-bridge inverter systems," IEEE Trans. Power Electron., vol. 21, no. 5, pp. 1385–1393, Sep. 2006.
- [14] F. Berba, D. Atkinson, and M. Armstrong, "Minimization of DC current component in transformer less Grid-connected PV inverter application," in Proc. 10th Int. Conf. Environ. Elect. Eng., Rome, Italy, May 2011, pp. 1–4.
- [15] Y. Shi, B. Liu, and S. Duan, "Eliminating DC current injection in current-transformer-sensed STATCOMs," IEEE Trans. Power Electron.,vol. 28, no. 8, pp. 3760–3767, Aug. 2013.
- [16] G. Buticchi, E. Lorenzani, and A. Fratta, "A new proposal to eliminate the DC current component at the point of common coupling for grid connected systems," in Proc. IEEE 36th Ann. Conf. Ind. Electron. Soc., Glendale, USA, Nov. 2010, pp. 3244–3249.
- [17] T.-F. Wu, H.-S. Nien, H.-M. Hsieh, and C.-L. Shen, "PV power injection and active power filtering with amplitude-clamping and amplitude-scaling algorithms," IEEE Trans. Ind. Appl., vol.43, no. 3, pp. 731–741, May/Jun. 2007.
- [18] W. M. Blewitt, D. J. Atkinson, J. Kelly, and R. A. Lakin, "Approach to low-cost prevention of DC injection in transformer less grid connected inverters," IET Power Electron., vol. 3, no. 1, pp. 111–119, Jan. 2010.